

Research Article

Effect of Zeolite Modification via Cationic Exchange Method on Mechanical, Thermal, and Morphological Properties of Ethylene Vinyl Acetate/Zeolite Composites

N. D. Zaharri, N. Othman, and Z. A. Mohd Ishak

School of Materials and Mineral Resources Engineering, Engineering Campus, Universiti Sains Malaysia, 14300 Nibong Tebal, Penang, Malaysia

Correspondence should be addressed to N. Othman; srnadras@eng.usm.my

Received 25 July 2013; Revised 16 October 2013; Accepted 19 October 2013

Academic Editor: Jim Low

Copyright © 2013 N. D. Zaharri et al. This is an open access article distributed under the Creative Commons Attribution License, which permits unrestricted use, distribution, and reproduction in any medium, provided the original work is properly cited.

In this research, organozeolite filled ethylene vinyl acetate (EVA) composites were prepared in a melt-mixing process and followed by compression molding using hot press machine according to standard test specimen. Prior to mixing process, zeolite was modified via cationic exchange of alkylammonium ions. The effect of zeolite or organozeolite loading from 5 up to 25 volume percentages on the properties of EVA/zeolite composites was evaluated. A combination of Fourier Transform Infrared Radiation (FTIR) and scanning electron microscopy (SEM) coupled with energy dispersive X-ray (EDX) analysis were done to characterize the resultant organoclay. Tensile test was performed in order to study the mechanical properties of the composites. EVA filled with organozeolite showed better tensile properties compared to EVA filled with unmodified zeolite, which might be an indication of enhanced dispersion of organophilic clay in the composites. Meanwhile, morphological study using SEM revealed the fibrillation effect of organozeolite. Besides, thermal properties of the composites were also characterized by using thermogravimetric analysis (TGA) and differential scanning calorimetry (DSC). The results showed that the application of the cation exchange treatment increases both decomposition and melting temperature of EVA/zeolite composites.

1. Introduction

There has been intensive research on layered silicate filled polymer composites recently. Several different layered silicates for polymer composites, for example, kaolinite, montmorillonite, hectorite, illite, muscovite, sepiolite, and hectorite, have been identified [1]. However until now, not much study has been done on natural zeolite, particularly mordenite type zeolite. Zeolite is another type of layered silicate material which can be classified into three groups according to Si/Al ratio in their frameworks, which are “low silica” zeolites, “intermediate silica” zeolites and also “high silica” zeolites [2]. Zeolites form a large group of hydrous silicates that show close similarities in composition, association, and mode of occurrence. The zeolite family includes mordenite, clinoptilolite, faujasite, chabazite, heulandite, and mazzite. They are framework aluminosilicates with exchangeable cations and highly variable amounts of H₂O in the generally large voids of the framework.

In this study, mordenite type zeolite is used as filler in polymer composites. Mordenite is classified into “intermediate silicate” zeolite where the Si/Al ratio is found to be between 4.5 and 5.5 [2]. Mordenites have been classified as “large-port” or “small-port,” depending on whether or not they adsorb large molecules such as benzene and cyclohexane. Ever since mordenite was synthesized, it has been known that some synthetic mordenite can accept cations or molecules larger than 4.5 Å, while natural mordenite cannot. Explanations for small-port mordenite have remained controversial [3]. Further varieties of mordenite can be produced by removing aluminum from the structure by strong acid treatment with hydrochloric acid [4].

Zeolites are widely known as microporous materials where each type of zeolite exhibits different pore structural characteristics. In the case of mordenite zeolite, the pore structure is complicated since the mordenite presents two types of porous channels. Figure 1 represents the channel

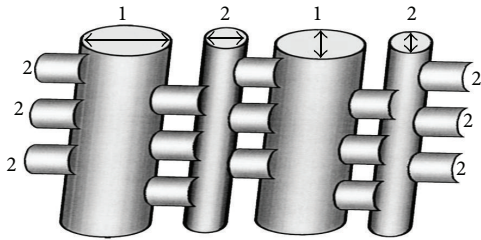


FIGURE 1: Channel structure of mordenite type zeolite [5].

structure of mordenite type zeolite. By referring to the figure, channel 1 is formed by the assemblage of 12-membered rings, each of which is having 12 oxygen atoms. Meanwhile channel 2 is made of 8-membered rings in which there are 8 oxygen atoms. Cation sites are located in the centers of this 8-membered rings channel [5]. The porous structure of mordenite consists of a channel system in which 8- and 12-membered ring channels run parallel to the [001] or c -axis and 8-membered run ones parallel to [010] or b -axis. Free diameters of the 12-membered rings are 0.65×0.70 nm, while free diameters of the 8-membered rings are 0.26×0.57 nm. Channels 1 and 2 are interconnected via perpendicular channel 2 tubes, in the form of small side pockets along the [010] axis. Thus the channel system is essentially a 2-dimensional network with elliptical 12-ring apertures and a limiting diffusion in the [010] or b direction [6].

However, the hydrophilic nature of inorganic mineral, including zeolites, limits its compatibility with polymer matrix. Hence, surface modification of filler needs to be done prior to compounding process in order to change the nature of filler from hydrophilic to hydrophobic. Enhancement of the polymer-filler interfacial adhesion by surface modification has become one of the popular evolutionary steps in polymer industry as well as in academic field. Compared to the unmodified composites, the composites filled with treated or modified filler exhibit increased mechanical properties, reduced gas permeability, and enhanced thermal stability and flame retardancy [7, 8].

In this study, method of cation exchange with alkylammonium ions was performed since it is the easiest way to make mineral fillers become hydrophobic yet effective in enhancing the properties of composites [9]. This cation exchange method does not only alter the surface polarity of the filler but also expand its intergallery distance, and thus it enables the polymer to penetrate more easily into the galleries. In the past several years, variety of fillers especially clays such as montmorillonite (MMT) [10], layered double hydroxides (LDH) [11], bentonite [12], and α -zirconium phosphate (α -ZrP) [13] have been ionic exchanged before being incorporated into polymer matrix in order to obtain optimal properties of composites.

However, there are only a few studies dealing with mordenite type zeolite modified by cationic exchange method in polymer composites. Zeolites are extensively used all over the world due to their ion exchange properties [14]. Due to this, zeolites can be easily modified using ion exchange treatment in order to change their nature from hydrophilic

to hydrophobic hence improving the compatibility between the inorganic filler particles and polymer matrix. In this treatment, the intercalated ions of zeolite are exchanged with the ions of organic surfactant which consequently alters the surface properties of zeolite to be hydrophobic. Among the widely used organic surfactants are phosphonium, imidazolium, stibonium compounds, and organic amines such as octadecylamine, hexadecylamine, dodecylamine, and octylamine. The swelling of mineral filler in aqueous surfactant, such as organic amine consisting alkylammonium ions, might lead to an extension of the interlayer galleries due to the hydration of inorganic ions contained in these galleries, allowing the alkylammonium ions to intercalate between them. However, some mineral fillers such as illites and kaolinites do not have expandable galleries due to strong interlayer interactions.

All clay minerals including zeolites show a main preference for larger over smaller inorganic cations. This tendency, referred to as "fixation" in the soil science literature, becomes more pronounced as layer charge increases. For smectites, this preference (for larger cations) follows the orders of $\text{Cs}^+ > \text{Rb}^+ > \text{K}^+ > \text{Na}^+ > \text{Li}^+$ and $\text{Ba}^{2+} > \text{Sr}^{2+} > \text{Ca}^{2+} > \text{Mg}^{2+}$. Meanwhile at higher layer charge (vermiculites), as in the case of mordenite type zeolite, the preference is $\text{Mg}^{2+} > \text{Ca}^{2+} \approx \text{Sr}^{2+} \approx \text{Ba}^{2+}$. The preference of clay minerals for certain cations is caused by several other effects. These include hydration of the cations at the surface and in solution (entropy), electrostatic cation-surface and cation-cation interactions, interaction between the water molecules and the surface, and the polarizability or hard and soft acid-base character of the cations [15].

The goal of this study was to improve the properties of EVA/zeolite composites by modifying the hydrophilic surface of zeolite using cation exchange method. FTIR and EDX analyses were done to elucidate the modification effect on the composites. The tensile properties and SEM analysis were evaluated in order to determine the mechanical and morphological properties of the composites, respectively. Also, thermogravimetric analysis (TGA) and differential scanning calorimetry (DSC) measurements were performed to characterize the thermal behavior of the EVA/zeolite composites.

2. Experimental

2.1. Materials. Ethylene vinyl acetate (EVA) containing 15% vinyl acetate was purchased from The Polyolefin Company (Singapore Pvt. Ltd. Cosmothene Eva H2020). The natural filler used was mordenite type of zeolite mineral species. The natural zeolite was mined in Indonesia. The chemical formula is $\text{Ca, Mg}_2, \text{K}_2 \text{Al}_2\text{Si}_{10}\text{O}_{24} \cdot 7\text{H}_2\text{O}$ with orthorhombic crystal system. It was provided in grains form and white color with density of 1.914 g/cm^3 . This filler was modified with octadecylamine with the chemical formula of $\text{CH}_3-(\text{CH}_2)_{17}-\text{NH}_2$. This product was purchased from Aldrich and used without further purification.

2.2. Cation Exchange Process. The octadecylamine was dissolved in 1 liter of 0.01 M hydrochloric acid solution (based

on deionized water). The solution was stirred at 80°C for few hours. Then 10 grams of zeolite were added to the solution which was then stirred at the same temperature for few more hours. The solution was then filtered and washed with hot ethanol : water (1 : 1) mixture. Finally, the resulting organoclay was then dried at 85°C for 36 hours and kept dry in a desiccator.

2.3. Preparation of the Composite. Prior to mixing process, zeolite was grinded into powder form using a ring mill machine. After grinding process, the exact particle size was determined by Malvern Mastersizer particle size analyzer. The result obtained was 5.62 μm . Then, the zeolite powder and EVA were dried in oven at 80°C for 24 hours. The compounding process was done by using an internal mixer Thermo Haake Polydrive with Rheomix, R600/610 model. The amounts of EVA and zeolite were calculated accurately according to Rules of Mixtures formula as shown in (1) [16].

Consider the following:

$$V_f = \frac{\rho_m W_f}{\rho_f W_m + \rho_m W_f}, \quad (1)$$

where V_f is volume percentage of filler and W_f and W_m are weight fraction of filler and matrix, respectively while ρ_f and ρ_m are density of filler and matrix, respectively.

The processing conditions were set at 130°C with 7 min of mixing time and 50 rpm of rotor speed. After compounding, the unmodified and modified zeolite filled composites were compression molded into 1 mm of sample thickness. The samples were preheated at 130°C for 8 minutes followed by compression for 2 minutes. Finally, the samples were cold pressed for 4 minutes.

2.4. Characterization. FTIR, PerkinElmer Spectrum One model machine, was used to investigate the presence of functional groups in zeolite, organozeolite, EVA/zeolite composite, and also EVA/organozeolite composite samples. The range of wavelength was 550–4000 cm^{-1} with 4 scan times. The standard spectrum was obtained from the FTIR machine in order to determine the involved functional groups.

The molded tensile test sheet for tensile testing was cut into five dumbbell-shaped samples using Wallace die cutter. The thickness of each dumbbell-shaped sample was measured. The tensile properties were determined using electromechanical Instron machine, model 3366 according to ASTM D 638 with a crosshead speed of 50 mm/min. The tensile mechanical properties such as tensile strength, elongation at break, and Young's modulus were obtained by calculating the average values of the five tested dumbbell-shaped samples.

Scanning electron microscopy/energy dispersive X-ray (SEM/EDX) analysis was performed using Leica Cambridge Ltd. model S360 to study the composites morphology. The morphology study was done on the fractured surface of the composite samples due to tensile testing. Samples were examined after sputter coating with gold to avoid electrostatic charging and poor image resolution. The relative amounts of occurrence elements in both unmodified and modified

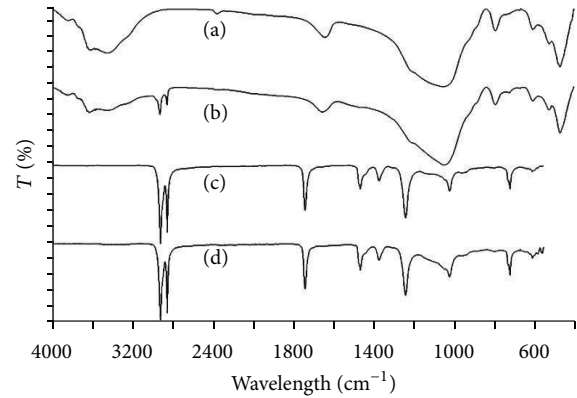


FIGURE 2: FTIR spectra of (a) zeolite, (b) organozeolite, (c) EVA/zeolite composite, and (d) EVA/organozeolite composite.

zeolite powder were measured using the energy dispersive X-ray analyzer facility of the microscope.

A PerkinElmer Pyris TGA-6 thermogravimetric analyzer was used to measure the weight losses and decomposition temperature of the EVA/zeolite composites in the temperature range of 20–600°C with a heating rate of 20°C/min and under a flow of nitrogen.

DSC was carried out with a PerkinElmer Pyris DSC-6 instrument to determine the crystallinity and melting temperature of the composites. Samples of EVA/zeolite composites were weighed to be approximately 5 mg and placed in an aluminum pan. DSC scans were obtained from 30–190°C at a rate of 10°C/min. The crystallinity degree for the composites is determined by the ratio $\Delta H_m / \Delta H_{m100}$, where ΔH_m is the heat of fusion in joule per gram polyethylene segments in the EVA samples, while ΔH_{m100} is the heat of fusion in joule per gram pure polyethylene with 100% crystallinity. The ΔH_{m100} is 281 joule per gram pure polyethylene with 100% crystallinity [17].

3. Results and Discussion

3.1. FTIR Analysis. FTIR spectra of unmodified and organomodified zeolite are illustrated in Figure 2. The common features in the FTIR spectra for zeolite and organozeolite are the presence of characteristics bands at around 3620, 1051, and 470 cm^{-1} which correspond to –OH stretching of structural hydroxyl group, Si–O stretching, and Al–O stretching, respectively. However, there are four new peaks present in the FTIR spectrum of organozeolite compared to the unmodified zeolite. The new peaks are 2918 and 2852 cm^{-1} which assigned to C–H asymmetric and symmetric stretching vibrations of surfactant, respectively meanwhile the new bands around 1468 and 3250 cm^{-1} are attributed to CH_2 methylene (scissoring) vibration and N–H stretching of alkyl ammonium, respectively. In addition, a reduction in intensity at 3620 cm^{-1} (–OH stretching peak) for organozeolite FTIR spectrum indicates that the zeolite becomes more organophilic or hydrophobic after the surface modification. For EVA/organozeolite composites, the spectrum shows a new broad absorption band at around 1070–1150 cm^{-1} in

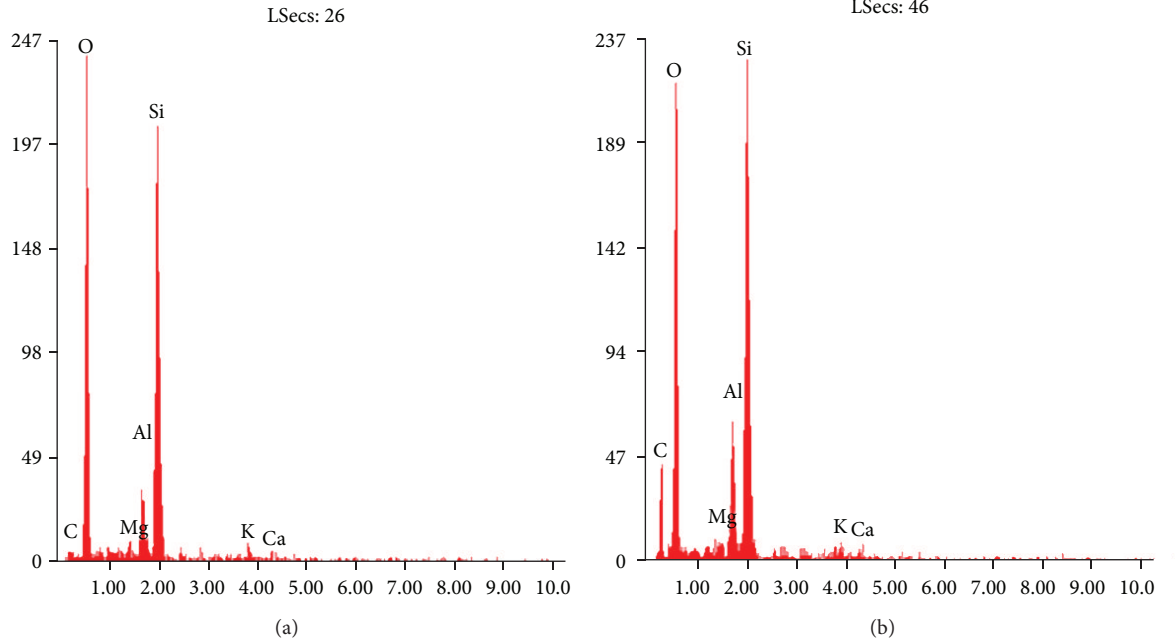


FIGURE 3: Semiquantitative elemental analysis provided by EDX.

TABLE 1: Weight percentages of occurrence elements in zeolite before and after modification.

Elements	Wt%	
	Zeolite	Organozeolite
O	42.34	34.81
Al	7.44	7.46
Si	41.31	32.62
C	3.66	21.20
Mg	1.53	0.73
K	2.56	1.62

comparison with EVA/zeolite composites. This new band which corresponded to the C–O–C group suggests the presence of possible reactions between acetate group of EVA and methyl group of octadecylamine. These prove that zeolite is successfully modified by the organic modifier (octadecylamine) and thus organozeolite is formed.

3.2. EDX Analysis. The semiquantitative elemental analysis provided by EDX detected several elements involved in creating the structure of zeolite which are Si, Al, O, C, Mg, and K as shown in Figures 3(a) and 3(b). It can be seen from the EDX spectrum that the bands of Mg and K reduced after surface modification. Moreover, the atomic ratio of C/Si changes from 0.0886 to 0.6499 in consequence of performing the cation exchange method. These clearly suggest the success of ion exchange on the expense of Mg^{2+} and K^+ cations and also the increment of C/Si atomic ratio. Table 1 represents the weight percentages of occurrence elements in unmodified and organozeolite powder.

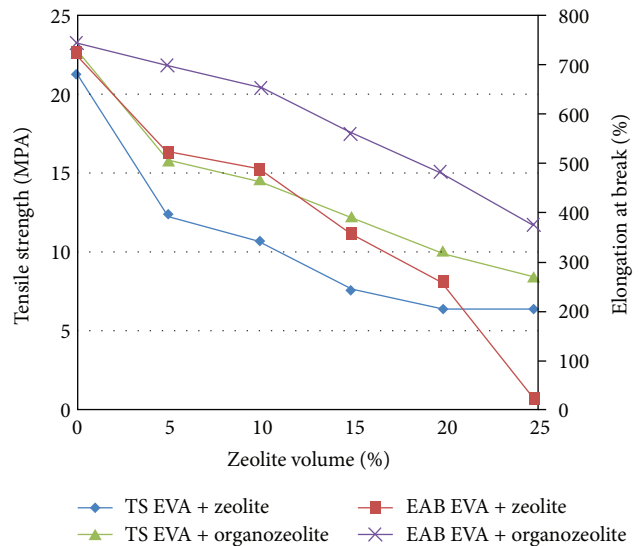


FIGURE 4: Tensile strength and elongation at break of zeolite and organozeolite EVA composites.

3.3. Tensile Properties. The tensile behavior of unmodified and organozeolite filled EVA composites at various zeolite content is presented in Figures 4 and 5. Figure 4 shows that tensile strength of both unmodified and modified composites decreased as the zeolite content was increased. This is due to the hydrophilic nature of zeolite which is incompatible with the hydrophobic EVA matrix. This leads to agglomeration and poor dispersion of zeolite in the EVA matrix hence reduced the composites strength at higher zeolite loading.

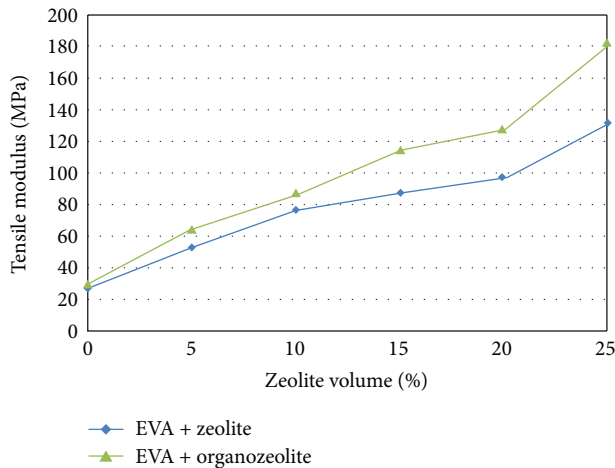


FIGURE 5: Tensile modulus of zeolite and organozeolite EVA composite.

Greater tensile strength can be observed for the composites filled with organozeolite compared to that of unmodified zeolite. The enhancement in tensile strength for organozeolite/EVA composites is attributed to the improved interaction between organozeolite and EVA matrix resulting from the cationic exchange reaction which has hydrophobilized the zeolite (as proved by FTIR and EDX results) hence enable it to be dispersed within the EVA matrix. It can also be inferred that this modification method has opened up the interlayer spaces of zeolite thus facilitating EVA matrix to penetrate between the layers. Furthermore, good interphase interaction between the dispersed zeolite and EVA matrix is believed to facilitate stress transfer from the continuous phase of EVA to the reinforcement phase of zeolite, hence allowing for tensile improvements. Similar results were reported by Velmurugan and Mohan for epoxy nanocomposites containing clay modified with alkyl quaternary ammonium [18].

Figure 4 also indicates that the elongation at break of EVA composites decreases with increasing zeolite content. This is probably due to the fact that ductility decreases when stiffness is increased by the incorporation of zeolite into the EVA matrix. However, the incorporation of organozeolite into EVA matrix results in higher elongation at break than that of unmodified zeolite at similar loading. This can be a consequence of enhanced adhesion between the organozeolite and EVA matrix thus increasing the ability of the composites to elongate before failure. The enhanced zeolite-EVA adhesion after the modification has also minimized the formation of voids, and hence deformations could not start so easily [19].

The addition of zeolite into EVA matrix significantly increases the tensile modulus of the composites as illustrated in Figure 5. This is due to the inherent properties of inorganic filler, which is rigid and has been proven to be efficient in stiffening polymers [20]. The tensile modulus of EVA/organozeolite composites is higher than that of EVA/zeolite composites at all filler content. This infers that

organozeolite is more compatible within EVA matrix compared to unmodified zeolite, which consequently increases the stiffness of the composites.

3.4. Morphology Study. Figures 6 and 7 show the tensile fracture surfaces of unmodified and organozeolite filled EVA composites, respectively. By comparing Figures 6(a) and 7(a), more extensive fibril structure morphology with minimal voids or cavities can be observed on the fractured surface of EVA/organozeolite composites. This indicates better adhesion and interfacial interaction formed between EVA matrix and organozeolite. Besides, the formation of fibrilous morphology indicates a more ductile failure compared to the unmodified composites [21]. This proves that, during deformation, the organozeolite absorbs more stress before fracture hence results in the significant improvement in tensile strength and elongation at break for the EVA/organozeolite composites. This result is in perfect agreement with those reported by Kocsis et al. (2004). At high zeolite loading (25 vol.%), the morphology of unmodified zeolite filled composites as shown in Figure 6(b) exhibits several agglomerations and voids which originate from poor interface adhesion between EVA matrix and zeolite [22]. Unlike Figure 7(b), almost no agglomeration and very little voids can be noticed in the morphology of EVA/organozeolite composites even at high zeolite loading (25 vol.%). This suggests that the surface modification of zeolite with octadecylamine is capable of increasing the compatibility between EVA matrix and organozeolite. These observations validate the results of tensile tests discussed earlier.

3.5. Thermogravimetric Analysis (TGA). Figures 8 and 9 illustrated the TGA and differential thermogravimetry (DTG) curves of EVA and its composites, respectively. The weight loss and derivative weight of EVA/zeolite composites caused by thermal degradation are monitored as a function of temperature. In general, the curve of thermal degradation of EVA is almost similar to that corresponding to its composites where 2 steps are presented. The first one is attributed to the vinyl acetate loss or deacetylation and the second one is associated with the decomposition of polyethylene chains resulting from the first process. As expected, the percentage of residue of zeolite content at completion of EVA degradation was found to increase with increasing zeolite loading in the matrix. It is also noted that EVA/zeolite composites exhibit higher weight loss at 600°C than that of EVA/organozeolite composites. This is because, at this temperature, the weight loss is corresponding to the dehydroxylation of zeolite [23]. This result also suggests that the EVA/organozeolite composite has been well hydrophobilized by cation exchanged method as shown by the lower reduction of weight at 600°C owing to the dehydroxylation process. Table 2 summarizes the selected parameters of thermal characteristics such as onset temperature, T_5 are taken as the point at which 5% degradation occurs, T_{90} indicating the temperature at 90% weight loss, and also T_{100} representing

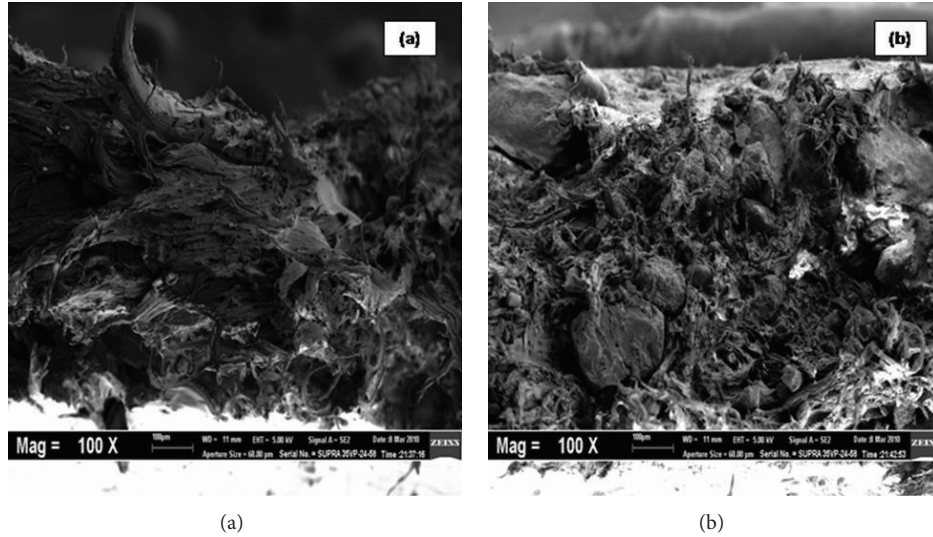


FIGURE 6: Tensile fracture surfaces of (a) 5 wt% EVA/zeolite and (b) 25 wt% EVA/zeolite.

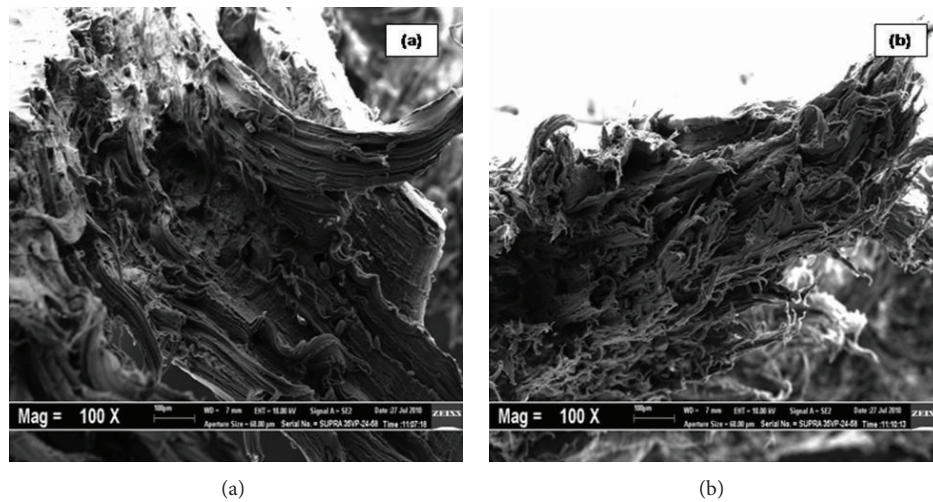


FIGURE 7: Tensile fracture surfaces of (a) 5 wt% EVA/organozeolite composite and (b) 25 wt% EVA/organozeolite composite.

the maximum degradation temperature of EVA and its composites. Surprisingly, the results demonstrate that the thermal stability of EVA decreased in the presence of both unmodified and organozeolite. This is in contrast with those reported by Alexandre and Dubois [24]. However, the reduction in T_5 , T_{90} , and also T_{100} with increasing zeolite content could be explained by the possibility of zeolite to accumulate heat and then be transformed as a heat source hence promotes an acceleration of the decomposition process in combination with the heat flow supplied by the outside heat source [25].

EVA/organozeolite composites exhibit greater T_5 and T_{90} compared to that of EVA/zeolite composites suggesting better interfacial interaction between EVA and organommodified zeolite. Also, the maximum degradation temperature (T_{100}) of organozeolite filled EVA composites is higher than that of unmodified composites. These results prove that the filler-matrix adhesion and also dispersion of filler within polymer

TABLE 2: TGA results of EVA matrix and its composites.

Composites system	T_5 ($^{\circ}\text{C}$)	T_{90} ($^{\circ}\text{C}$)	T_{100} ($^{\circ}\text{C}$)
EVA	367	447	497
5% EVA/zeolite	328	440	488
15% EVA/zeolite	293	412	458
25% EVA/zeolite	247	397	441
5% EVA/organozeolite	338	447	496
15% EVA/organozeolite	321	416	462
25% EVA/organozeolite	315	401	445

matrix are important factors governing the thermal stability of the composites. Similar results were obtained by Zhang et al. (2003) where they reported that the well-dispersed filler in the polymer matrix could be more effective in

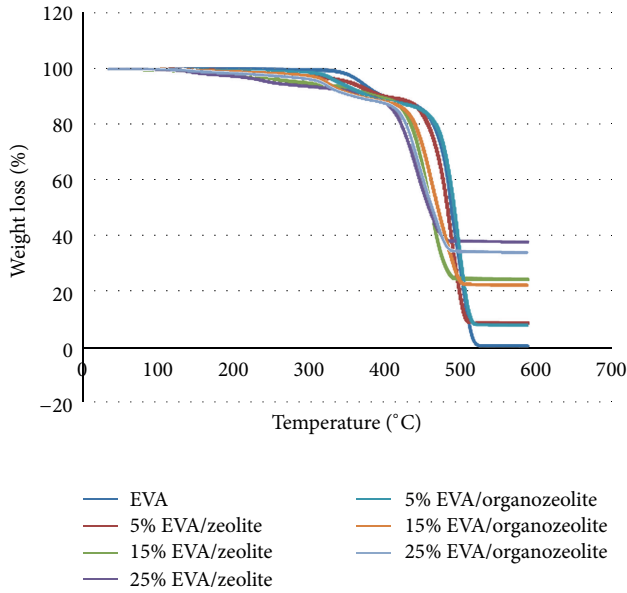


FIGURE 8: TGA curves of zeolite and organozeolite EVA composites.

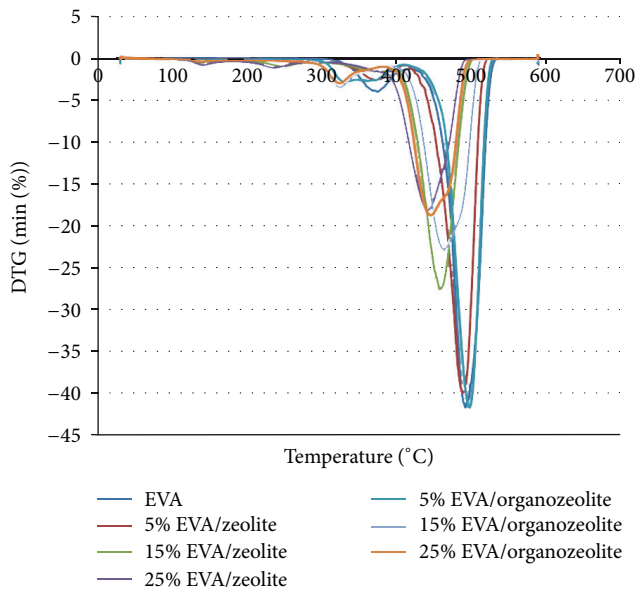


FIGURE 9: Thermogravimetry (DTG) curves of zeolite and organozeolite EVA composites.

hindering the diffusion of volatile decomposition products hence leading to the improved thermal stability [26].

3.6. *Differential Scanning Calorimetry (DSC).* Figure 10 indicates the DSC thermograms of unmodified and organozeolite filled EVA composites with different zeolite contents. As shown in the figure, pure EVA is melted at 91.46°C and the melting temperature decreased with the addition of zeolite. The same reason as explained in the result of TGA could be used to account for the decreased thermal

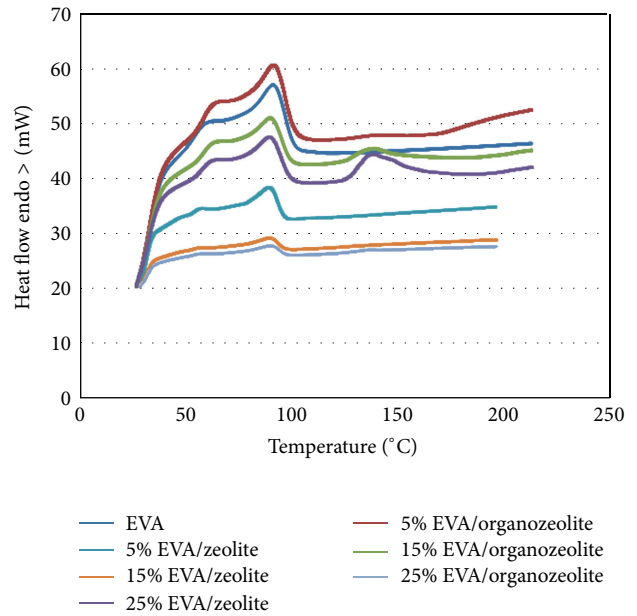


FIGURE 10: The DSC thermograms of unmodified and organozeolite filled EVA composites with different zeolite contents.

TABLE 3: DSC results of EVA matrix and its composites.

Composites system	Melting temperature (°C)	Enthalpy of fusion (J/g)	Degree of crystallinity (%)
EVA	92	29	10
5% EVA/zeolite	89	27	10
15% EVA/zeolite	89	19	7
25% EVA/zeolite	89	16	6
5% EVA/organozeolite	92	21	7
15% EVA/organozeolite	90	19	7
25% EVA/organozeolite	90	15	5

stability in the presence of zeolite. However, the reduction in melting temperatures with increasing zeolite loading is not significant. The DSC measurements show that the incorporation of organozeolite into EVA matrix results in higher melting temperature relative to the unmodified zeolite filled EVA composites. This is believed to be due to the improved interfacial interaction between EVA and organozeolite, resulting from the cation exchange method treatment. Table 3 lists the melting temperature and the degree of crystallinity of EVA composites. Poly (vinyl acetate) segment in the EVA copolymer is assumed to be noncrystalline in the calculation of the percent crystallinity of the sample. Apparently, the incorporation of both unmodified and organozeolite into EVA matrix reduced the heat of fusion which leads to lower degree of crystallinity. Probably, this is due to the presence of zeolite causing physical hindrance to the motion of EVA molecular chains hence retarding the crystallization of polymer phase of the composites which consequently reduces the degree of crys-

tallinity [27]. It can also be seen from the table that EVA/organozeolite composites possess lower crystallinity than that of EVA/zeolite composites. This might be attributed to the improved interaction between EVA and organozeolite providing greater effect in imparting physical hindrance to restrict the molecular chain mobility of EVA.

4. Conclusions

It can be concluded that the surface modification of zeolite by organic modifier (octadecylamine) is capable of improving the properties of EVA/zeolite composites. FTIR and EDX results revealed that zeolite has been successfully modified via cation exchange method. Incorporation of both unmodified and organozeolite increased the stiffness but decreased the strength and ductility of EVA matrix. However, EVA/organozeolite composites show higher value of tensile strength, elongation at break, and tensile modulus than those of unmodified zeolite filled EVA composites. This might be attributed to the improved compatibility between EVA and organomodified zeolite. SEM micrographs also supported the finding of improved compatibility for the EVA/organozeolite through a better dispersion of the organozeolite within EVA matrix hence gives an improvement in the composites properties. TGA and DSC results indicate that the thermal properties of EVA decreased in the presence of both zeolite and organozeolite. Organozeolite filled EVA composites exhibit higher melting and thermal decomposition temperature compared to that of unmodified zeolite filled EVA composites.

Acknowledgments

The authors thank Universiti Sains Malaysia for a Research University Grant (no. 1001/PBAHAN/8033027) which financially supported this work. Gratitude is also expressed to all the academic and nonacademic staff in the School of Materials and Mineral Resources Engineering for their support and contribution to the project.

References

- [1] S. M. Auerbach, K. A. Carrado, and P. K. Dutta, *Handbook of Layered Materials*, CRC, 2004.
- [2] F. R. Ribeiro, *Zeolites—Science and Technology*, vol. 80, Springer, 1984.
- [3] L. B. Sand, "Synthesis of large-pore and small pore mordenites," in *Molecular Sieves*, Society of Chemical Industry, London, UK, 1968.
- [4] M. M. Dubinin, "Porous structure of adsorbents and catalysts," *Advances in Colloid and Interface Science*, vol. 2, no. 2, pp. 217–235, 1968.
- [5] K. Ssing, D. Everett, R. Haul et al., "Reporting physisorption data for gas/solid system," *Pure and Applied Chemistry*, vol. 57, no. 4, pp. 603–619, 1985.
- [6] P. A. Jacobs and J. A. Martens, *Synthesis of High-Silica Aluminosilicate Zeolites*, vol. 33, Elsevier Science Limited, 1987.
- [7] A. Usuki, A. Koiwai, Y. Kojima et al., "Interaction of nylon 6-clay surface and mechanical properties of nylon 6–clay hybrid," *Journal of Applied Polymer Science*, vol. 55, no. 1, pp. 119–123, 2003.
- [8] E. M. Araújo, R. Barbosa, A. W. B. Rodrigues, T. J. A. Melo, and E. N. Ito, "Processing and characterization of polyethylene/Brazilian clay nanocomposites," *Materials Science and Engineering A*, vol. 445, pp. 141–147, 2007.
- [9] G. Lagaly, "Characterization of clays by organic compounds," *Clay Minerals*, vol. 16, no. 1, pp. 1–21, 1981.
- [10] S. Chuayjuljit, R. Thongraar, and O. Saravari, "Preparation and properties of PVC/EVA/ organomodified montmorillonite nanocomposites," *Journal of Reinforced Plastics and Composites*, vol. 27, no. 4, pp. 431–442, 2008.
- [11] M. Badreddine, A. Legrouri, A. Barroug, A. de Roy, and J. P. Besse, "Ion exchange of different phosphate ions into the zinc-aluminum-chloride layered double hydroxide," *Materials Letters*, vol. 38, no. 6, pp. 391–395, 1999.
- [12] S. Chandramouleeswaran and S. T. Mhaske, "Novel tailored polymeric surfactant for dispersing clay into the non polar polymer," *Journal of Dispersion Science and Technology*, vol. 29, no. 7, pp. 1024–1028, 2008.
- [13] H. Wu, C. Liu, J. Chen, Y. Yang, and Y. Chen, "Preparation and characterization of chitosan/ α -zirconium phosphate nanocomposite films," *Polymer International*, vol. 59, no. 7, pp. 923–930, 2010.
- [14] G. P. Tsintskaladze, A. R. Nefedova, Z. V. Gryaznova, G. V. Tsitshishvili, and N. G. Gigolashvili, "Active centres of decationated zeolites in oxidative transformation of methanol," *Petroleum Chemistry*, vol. 25, no. 3, pp. 160–165, 1985.
- [15] M. Auboiroux, F. Melou, F. Bergaya, and J. C. Touray, "Hard and soft acid-base model applied to bivalent cation selectivity on a 2:1 clay mineral," *Clays and Clay Minerals*, vol. 46, no. 5, pp. 546–555, 1998.
- [16] M. Xanthos, *Functional Fillers for Plastics*, Wiley-Vch, 2010.
- [17] R. Z. Greenley, J. Brandrup, and E. Immergut, "Polymer handbook," in *Polymer Handbook*, pp. 267–274, 1989.
- [18] R. Velmurugan and T. P. Mohan, "Room temperature processing of epoxy-clay nanocomposites," *Journal of Materials Science*, vol. 39, no. 24, pp. 7333–7339, 2004.
- [19] H. Demir, D. Balköse, and S. Ülkü, "Influence of surface modification of fillers and polymer on flammability and tensile behaviour of polypropylene-composites," *Polymer Degradation and Stability*, vol. 91, no. 5, pp. 1079–1085, 2006.
- [20] J. Wang and R. Pyrz, "Prediction of the overall moduli of layered silicate-reinforced nanocomposites-part I: basic theory and formulas," *Composites Science and Technology*, vol. 64, no. 7, pp. 925–934, 2004.
- [21] P. W. Balasuriya, L. Ye, and Y.-W. Mai, "Morphology and mechanical properties of reconstituted wood board waste-polyethylene composites," *Composite Interfaces*, vol. 10, no. 2-3, pp. 319–341, 2003.
- [22] W. S. Chow, Z. A. M. Ishak, U. S. Ishiaku, J. Karger-Kocsis, and A. A. Apostolov, "The effect of organoclay on the mechanical properties and morphology of injection-molded polyamide 6/ polypropylene nanocomposites," *Journal of Applied Polymer Science*, vol. 91, no. 1, pp. 175–189, 2004.
- [23] H. van Olphen and J. Fripiat, *Data Handbook for Clay Minerals and Other Non-Metallic Materials*, Pergamon Press, New York, NY, USA, 1979.
- [24] M. Alexandre and P. Dubois, "Polymer-layered silicate nanocomposites: preparation, properties and uses of a new class of materials," *Materials Science and Engineering R*, vol. 28, no. 1, pp. 1–63, 2000.

- [25] S. S. Ray and M. Okamoto, "Polymer/layered silicate nanocomposites: a review from preparation to processing," *Progress in Polymer Science*, vol. 28, no. 11, pp. 1539–1641, 2003.
- [26] W. Zhang, Y. Liang, W. Luo, and Y. Fang, "Effects of clay-modifying agents on the morphology and properties of poly(methyl methacrylate)/clay nanocomposites synthesized via γ -ray irradiation polymerization," *Journal of Polymer Science A*, vol. 41, no. 21, pp. 3218–3226, 2003.
- [27] H. M. Jeong, B. C. Kim, and E. H. Kim, "Structure and properties of EVOH/organoclay nanocomposites," *Journal of Materials Science*, vol. 40, no. 14, pp. 3783–3787, 2005.



Hindawi

Submit your manuscripts at
<http://www.hindawi.com>

